Journal of Biomedical Optics

SPIEDigitalLibrary.org/jbo

Method for depth-resolved quantitation of optical properties in layered media using spatially modulated quantitative spectroscopy

Rolf B. Saager
Alex Truong
David J. Cuccia
Anthony J. Durkin

SPIE

Method for depth-resolved quantitation of optical properties in layered media using spatially modulated quantitative spectroscopy

Rolf B. Saager,[a] Alex Truong,[a] David J. Cuccia,[b] and Anthony J. Durkin[a]
[a]University of California-Irvine, Beckman Laser Institute, 1002 Health Sciences Road, Irvine, California 92612
[b]Modulated Imaging, Inc., 1002 Health Sciences Road, Irvine, California 92612

Abstract. We have demonstrated that spatially modulated quantitative spectroscopy (SMoQS) is capable of extracting absolute optical properties from homogeneous tissue simulating phantoms that span both the visible and near-infrared wavelength regimes. However, biological tissue, such as skin, is highly structured, presenting challenges to quantitative spectroscopic techniques based on homogeneous models. In order to more accurately address the challenges associated with skin, we present a method for depth-resolved optical property quantitation based on a two layer model. Layered Monte Carlo simulations and layered tissue simulating phantoms are used to determine the efficacy and accuracy of SMoQS to quantify layer specific optical properties of layered media. Initial results from both the simulation and experiment show that this empirical method is capable of determining top layer thickness within tens of microns across a physiological range for skin. Layer specific chromophore concentration can be determined to $< \pm 10\%$ the actual values, on average, whereas bulk quantitation in either visible or near infrared spectroscopic regimes significantly underestimates the layer specific chromophore concentration and can be confounded by top layer thickness. [DOI: 10.1117/1.3597621]

Keywords: spectroscopy; tissues; turbid media; spatial frequencies; reflectance.

Paper 11119R received Mar. 10, 2011; revised manuscript received Apr. 15, 2011; accepted for publication May 16, 2011; published online Jul. 7, 2011.

1 Introduction

Quantitative optical spectroscopy can be a useful tool for non-invasively characterizing the properties of *in vivo* biological tissues. In particular, the absorption properties quantified by these techniques can be directly correlated to physiologically relevant chemical species, such as oxygenated and deoxygenated hemoglobin, melanin, lipid, and water concentrations. These techniques typically separate and quantify the effects of absorption from that of the scattering of light due to cellular and extracellular structures that comprise the tissue by exploiting the spatial, temporal, and/or the spectral dependence of light as it travels through turbid media such as tissue. These spectroscopic instruments can interrogate the optical properties of tissue in either the visible[1,2] or near-infrared regimes.[3] Recently, spectroscopic approaches have been proposed that are capable of spanning both visible and near-infrared regimes either through spatial domain[4] or spatial frequency domain[5] techniques. Though the depth sensitivities and resolution of these techniques may vary due to the choice of wavelength regime or the spatial/temporal characteristics of the source, they typically model light transport in tissue as a homogeneous semi-infinite medium and therefore, the reported absorption coefficient is generally a volume averaged quantity.

Biological tissues such as skin, however, are highly structured and layered. Chromophores such as melanin, are typically confined within the epidermis, whereas hemoglobin is confined within the dermis beneath. When quantitative spectroscopic techniques interrogate the skin, the resulting optical properties represent contributions from both layers. Since these techniques typically interpret measurements as bulk optical properties from a homogeneous volume, several issues arise as these approaches are 1. dependent on the depth sensitivity of the specific technique used to measure, and 2. variations in epidermal thickness can confound determination of chromophore concentration by altering the partial volume sensitivity to each layer. Since the optical properties of skin (both in terms of absorption and reduced scattering coefficient) are higher in the visible regime relative to these properties in the near-infrared, visible regime spectroscopy of skin reports that optical properties that are more heavily weighted toward the properties of the epidermis and near-infrared techniques are more weighted toward properties of the dermis. Spatially modulated quantitative spectroscopy (SMoQS), as we practice it, is a quantitative technique that spans both visible and near-infrared regimes and as a result, is able to probe a range of depths into tissue as a function of the wavelengths employed; embedding both chromophore and depth information across the spectral range of data.

Diffusion-based models in the frequency domain and previous studies in spatial frequency domain (SFD) have explored the temporal or spatial frequency dependence of optical depth penetration to determine layer thickness and layer specific optical properties in the near-infrared.[6,7] Here, we present a simple, empirical approach to interpreting the wavelength dependent weighting of depth sensitivity and utilizing this relative sensitivity difference in visible and near-infrared regimes to determine epidermal thickness and to isolate layer specific concentrations. Through this approach, the ambiguity between

Address all correspondence to: Rolf Saager, University of California-Irvine, Beckman Laser Institute, 1002 Health Sciences Road, Irvine, California 92612. Tel: 949 824 4104; Fax: 949 824 4868; E-mail: rsaager@uci.edu.

1083-3668/2011/16(7)/077002/8/$25.00 © 2011 SPIE

layer specific chromophore concentration and layer thickness can be mitigated.

2 Methods

2.1 *Instrumentation*

SFD techniques were first demonstrated in 1998, using a laser as the illumination source.[8] The principles underlying the extraction of absorption and reduced scattering coefficients using a SFD approach have recently been enumerated in detail elsewhere.[9] In general, this approach quantifies the modulation transfer function (MTF) of a medium by projecting sinusoidal intensity patterns of light at several different spatial frequencies. In this case, the turbid sample, such as tissue, becomes the medium under test. The captured spatially modulated reflectance is then modeled using either the diffusion theory or Monte Carlo simulations in order to deduce absorption and reduced scattering coefficients. As shown by Cuccia et.al.,[9] the relative contribution of absorption and reduced scattering to the spatially modulated reflectance varies as a function of spatial frequency. By modeling this relationship at multiple spatial frequencies through the diffusion theory or Monte Carlo simulations, the quantitative absorption and reduced scattering coefficients can be uniquely deduced.

While previously reported SFD techniques have focused on wide-field quantitative imaging at several discrete wavelengths, SMoQS executes this method at a relatively small single location (1-mm spot size), trading image resolution for a broader spectral range and resolution (430 to 1050 nm and ~1 nm, respectively). Since SMoQS includes visible wavelengths, the diffusion approximation breaks down requiring Monte Carlo methods to model the spatial frequency dependence of the spatially modulated reflectance across all wavelengths detected.

We have developed instrumentation to execute SMoQS by projecting sinusoidal intensity patterns of a broadband source onto turbid samples or tissue under interrogation (schematically shown in Fig. 1). We use a 250 W tungsten-halogen lamp (Newport Optics) for the broadband illumination source and a digital micro-mirror device (DMD) (DLP developers kit, Texas Instruments) to spatially modulate the light intensity. The DMD is imaged onto the target tissue or sample, resulting in programmable spatial frequency patterns that are projected over a 26×34 mm^2 field of view.

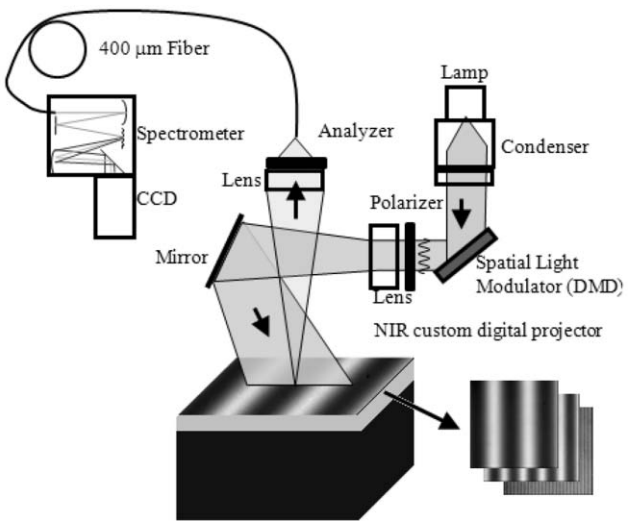

Fig. 1 SMoQS system diagram.

Collection optics image a 1-mm diameter spot from the center of the field of view onto the distal end of a 400 μm core fiber. The diffusely reflected light collected by this detector fiber is delivered to the entrance slit of a tunable grating Oriel spectrograph (model no. 77480). For our purposes, this spectrograph is tuned to cover a range of 430 to 1050 nm, with ~1 nm spectral resolution. A 16-bit, TEC controlled CCD (Instaspec IV, Oriel) was used to detect the chromatically dispersed light. Additionally, a crossed, 2 in., wire grid polarizer/analyzer pair are placed in the instrument to reject any specularly reflected light from reaching the spectrometer. In this system, the polarizer is positioned between the DMD and the projection optics, whereas the analyzer is positioned between the collection optics and the detector fiber.

Both DMD and CCD were computer controlled through a LABVIEW platform, allowing for automated data acquisition over a specified number of spatial frequencies. An auto-exposure subroutine was developed to optimize the dynamic range of the CCD specific to the amount of diffusely reflected light collected from sample of interest. Though this system is not fully optimized for light throughput, the auto-exposure routine currently sets acquisition times that currently range from 0.1 to 0.6 s per pattern projected, depending on the optical properties of the sample of interest. In terms of skin tissue, this brackets the range of acquisition times needed to collect light with acceptable signal-to-noise ratio from relatively highly reflecting fair skin to highly absorbing pigment moles.

Currently, 7 spatial frequencies are acquired, ranging from 0 to 0.35 mm^{-1}. This range was chosen to encompass the range of absorption sensitivity as a function of spatial frequency, (i.e., whereas the 0 mm$-^{1}$ frequency reflectance holds the greatest sensitivity to the effects of absorption, 0.35 mm^{-1} frequency reflectance is nearly exclusively due to reduced scattering). In order to extract the spatial frequency dependent reflectance (i.e., the ac component of the signal), a 3-phase demodulation scheme is employed.[5] This requires 3 evenly spaced phases (0, 120, and 240 deg) of each spatial frequency to be projected. As a result, for the instrument's current deployment, 21 total patterns are projected and acquisition times for the entire sequence range from 2 to 30 s. Calibration measurements were also collected from a turbid reflectance standard to correct the demodulated spectra for instrumentation artifacts. Spatial frequency dependent tissue reflectance at individual wavelengths is then fit to homogeneous Monte Carlo models to produce unique pairs of absorption and reduced scattering. It is important to note that this method for determining optical properties is still dependent on a homogeneous model, yet these results can still be exploited as the depth sensitivity of the changes across the broad range of wavelengths employed in this system.

2.2 *Model*

For our initial model, we define the epidermis as the top layer of our model and that it exclusively contains melanin, whereas the dermis contains both oxy- and deoxy-hemoglobin. Here, we

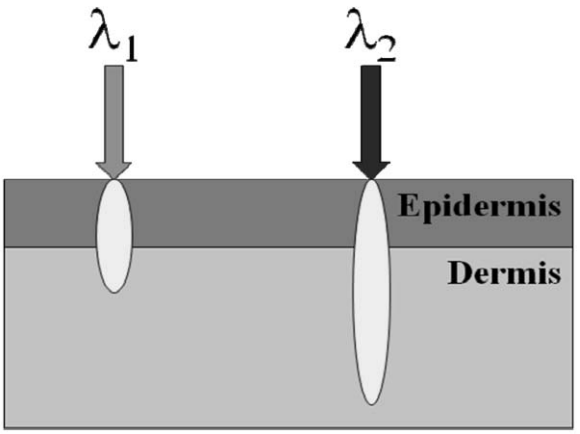

Fig. 2 Two layer model for skin. Here, the top layer represents the bulk optical properties (absorption and reduced scattering) of the epidermis and the bottom layer represents the properties of the dermis. Our model assumes that each wavelength of light will interrogate both layers; however, the relative contribution from each layer will vary as a function of the wavelength dependent interrogation depth.

assume that the optical properties of the epidermis and dermis are separate and distinct. Since the epidermal thickness typically ranges from 60 to 300 μm,[10,11] our model assumes that all wavelengths in our range of interest penetrate through the epidermis and hence, the diffuse reflectance detected from the skin contains contributions from both epidermal and dermal layers, shown schematically in Fig. 2.

In the context of this model, quantitative spectroscopic measurements of tissue represent partial contributions from each layer. In general, the absorption values determined from any quantitative spectroscopic technique like SMoQS can be interpreted as the linear superposition of absorption from each layer, scaled by the optical pathlength traveled specific to each layer. Since SMoQS is based on a planar illumination scheme, photon transport can be simplified and represented in one dimension, in terms of depth, which is dependent on the optical properties of the tissue. In this particular case, there is a direct relationship between optical properties for a given wavelength and depth into tissue that it interrogates. The relative contributions from each layer to the total measured absorption can now be modeled in terms of the one-dimensional depth interrogated by photons as they pass through the tissue volume, shown in Eq. (1):

$$\mu_{a\_\mathrm{meas}}(\lambda)\, l_{\mathrm{meas}}(\lambda) = c_1 \mu_{a1}(\lambda)\, l_1 + c_2 \mu_{a2}(\lambda)\, l_2(\lambda). \quad (1)$$

Here, the total depth interrogated by the measurement, l_{meas}, is the sum of depths interrogated in each layer. Since we make the assumption that all wavelengths in the 450 to 1050 nm range penetrates through the top layer, l_1, is a constant; however, l_2 represents the additional depth interrogated. l_2 is dependent on the bulk optical properties of the tissue and hence is permitted to vary as a function of wavelength.

$$l_{\mathrm{meas}}(\lambda) = l_1 + l_2(\lambda). \quad (2)$$

Likewise, the measured concentration from each layer can be interpreted as the layer-specific concentration, scaled by the relative depth interrogated in that layer to the total depth measured.

$$c_{1\mathrm{meas}}(\lambda) = c_1 \left(\frac{l_1}{l_{\mathrm{meas}}(\lambda)} \right),$$

$$c_{2\mathrm{meas}}(\lambda) = c_2 \left(\frac{l_2}{l_{\mathrm{meas}}(\lambda)} \right) = c_2 \left(\frac{l_{\mathrm{meas}}(\lambda) - l_1}{l_{\mathrm{meas}}(\lambda)} \right). \quad (3)$$

If the measured concentrations specific to the chromophores in each layer and the depth of interrogation can be estimated at two wavelength regimes with distinctly different optical properties, the top layer thickness, l_1, can be determined as well as the layer-specific concentrations, c_1 and c_2.

$$l_1 = \frac{[c_{2\mathrm{meas}}(\lambda_1) - c_{2\mathrm{meas}}(\lambda_2)]\, l_{\mathrm{meas}}(\lambda_1)\, l_{\mathrm{meas}}(\lambda_2)}{[c_{2\mathrm{meas}}(\lambda_1)\, l_{\mathrm{meas}}(\lambda_1) - c_{2\mathrm{meas}}(\lambda_2)\, l_{\mathrm{meas}}(\lambda_2)]}. \quad (4)$$

From SMoQS, quantitative absorption and reduced scattering coefficient values can be determined for bulk tissue. Though these measured quantities do not directly reflect layer specific optical properties, they can be employed to estimate $l_{\mathrm{meas}}(\lambda)$, $c_{1\,\mathrm{meas}}(\lambda)$, and $c_{2\mathrm{meas}}(\lambda)$. For this initial investigation, we use a classic planar illumination definition of penetration depth, δ,[12] as our estimate for $l_{\mathrm{meas}}(\lambda)$. Since δ reports depth in terms of optical depth, we scale this value by the index of the refraction of tissue, n_{tissue}, assumed to be 1.4 for this study, to relate this calculation to physical depth:

$$l_{\mathrm{meas}}(\lambda) = \frac{\delta(\lambda)}{n_{\mathrm{tissue}}} = \frac{1}{n_{\mathrm{tissue}} \mu_{\mathrm{eff}}(\lambda)}$$

$$= \frac{1}{n_{\mathrm{tissue}} \sqrt{3\mu_a(\lambda)\,(\mu_a(\lambda) + \mu_s'(\lambda))}}. \quad (5)$$

To estimate the wavelength dependent chromophore concentration, a linear, least-squares fit of assumed chromophore basis sets can be performed over a spectral window, centered at any given wavelength. While there can be much discussion regarding the optimal window size or the specific number of discrete wavelengths necessary to provide optimal separation of constituent chromophores through a least-squares minimization, this initial investigation will only consider using discrete spectral windows in either visible or near infrared regimes to illustrate the potential of this approach. To match the range of wavelengths employed to determine the constituent chromophore concentrations, the averaged penetration depth over the same spectral window is used.

3 Data Analysis and Results

3.1 *Simulated Data*

First, we will use computer simulated data to work through a synthetic two layered system. Simulated SMoQS measurements were generated using multilayer Monte Carlo (MCML) methods.[13] From the MCML core code, spatially resolved (i.e., spatial domain) reflectance from a pencil beam source can be modeled. Since the spatial and spatial frequency domains are Fourier conjugates of each other, spatial frequency dependent reflectance values [$R(f_x)$] can be generated from the spatially domain reflectance results [R(x)]. MCML, however, exploits cylindrical symmetry to reduce the computational demand for these simulations and therefore, a simple Fourier transform does not account for the geometric symmetry of the code. Instead, a Hankel transform is employed since it does account for cylindrical symmetry and has been shown to accurately

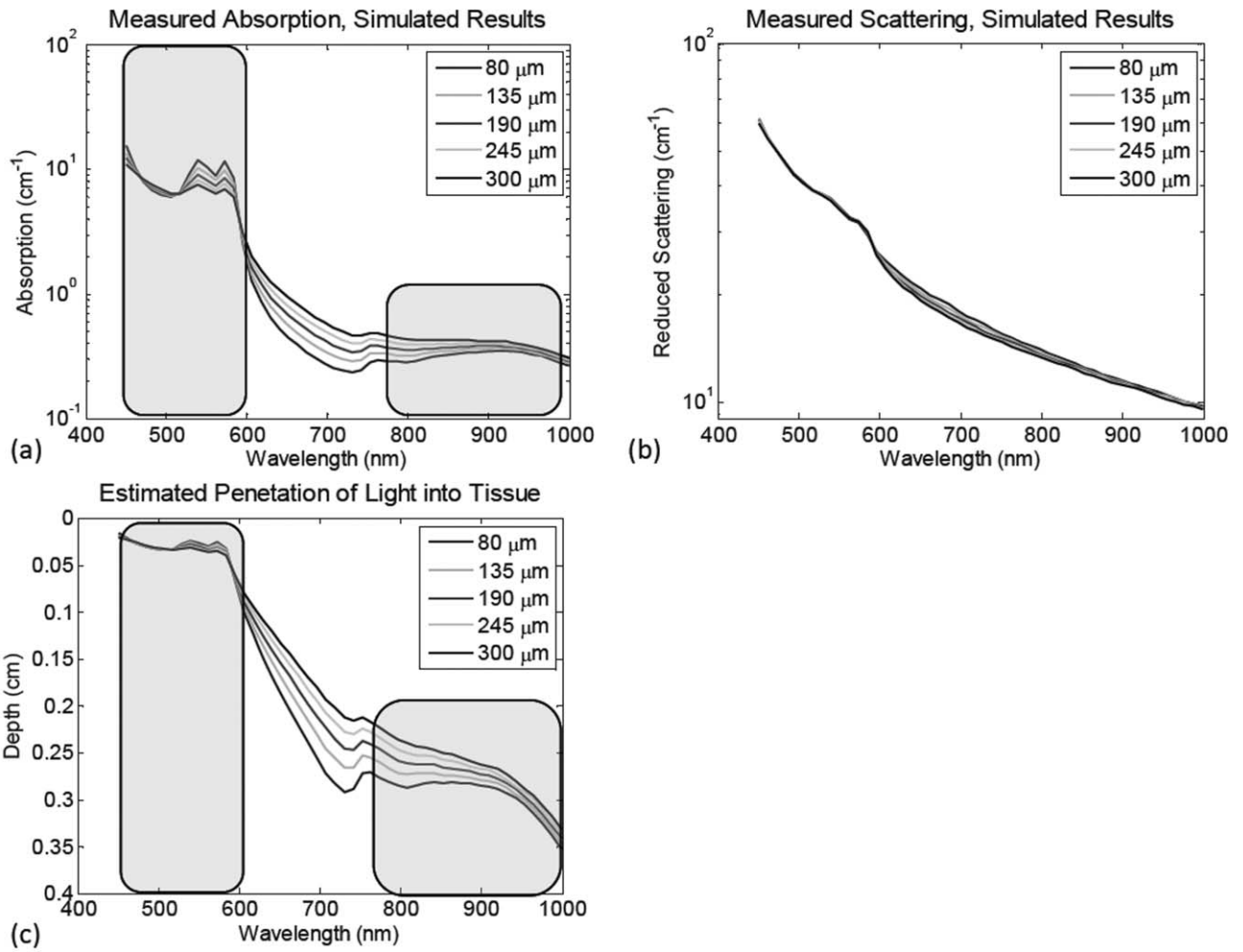

Fig. 3 Simulated results. (a) The resulting absorption spectra from the simulated two layer construct, as processed by a standard homogeneous model based spatial frequency domain algorithm. (b) The resulting reduced scattering spectra from the two layer phantom constructs. (c) The calculated optical penetration depth based off of the wavelength specific determined absorption and reduced scattering values. Highlighted regions indicate the spectral windows used to determine the top layer thickness, per Eq. (5).

transform spatial and spatial frequency domains under these conditions.[9]

To model skin, a reference absorption spectrum of melanin[14] is used for the top layer and oxy- and deoxy- hemoglobin spectra are used for the bottom layer.[15] To approximate normal skin, a 1% concentration of melanin (per volume of the epidermis) was used and 5% hemoglobin at 80% oxygenation was used to model the microvascular bed of the dermis. Scattering in both layers was modeled empirically by a two-part power-law approach proposed by Jacques,[16] where $D = 42\ \mathrm{cm}^{-1}$ and $f = 0.62$ represent scattering parameters for skin.

$$\mu_s'(\lambda) = D\left[f\left(\frac{\lambda}{500\,\mathrm{nm}}\right)^{-4} + (1-f)\left(\frac{\lambda}{500\,\mathrm{nm}}\right)^{-1}\right]. \tag{6}$$

The layer specific optical properties were inputs to the Monte Carlo routine at 50 wavelengths spanning 450 to 1000 nm. Each wavelength specific set of optical properties was also run across 5 different layer thicknesses, which in this study, ranged from 80 to 300 μm. In the end, a simulated measurement data set is generated, where broadband absorption and scattering properties can be determined from spatial frequency domain methods for 5 epidermal layer thicknesses at ~12 nm resolution for the same set of melanin and hemoglobin concentrations.

Figure 3(a) shows the difference in the determined absorption properties that result from the variation in layer thickness. Figure 3(b) shows the determined reduced scattering. The additional structure present in these results (particularly noticeable in the 500 to 600 nm range). Since these values are determined from a homogeneous model, there is some cross-talk error due to the layer specific properties, however, this represents >6% error in the determination of the quantitative scattering values. The estimated depth penetration as a function of wavelength is shown in Fig. 3(b). By selecting two spectral regimes (450 to 605 nm and 784 to 1000 nm), wavelength specific concentrations and penetration depths can be estimated from the determined optical properties and hence, the top layer thickness and layer-specific absorption concentration can be determined. Table 1 summarizes the results of this partial volume model approach. These results illustrate that the determination of the top layer thickness produces values that are within tens of micrometers to the actual values. However, this error appears to exhibit some dependence of the layer thickness itself, which may have to do with our use of optical depth penetration metrics as a proxy for

Table 1 Simulated results.

Layer thickness (μm)		Melanin (1.0%)		HbO_2 (4.0%)		Hb (1.0%)	
Actual	Calc.	Calc.	Vis/NIR only	Calc.	Vis/NIR only	Calc.	Vis/NIR only
80	**81**	**0.95**	0.21/0.05	**4.05**	3.1/3.9	**1.01**	0.48/1.01
135	**136**	**0.96**	0.34/0.08	**4.03**	2.4/3.7	**1.12**	0.25/1.08
190	**181**	**0.99**	0.45/0.11	**4.00**	1.8/3.6	**1.19**	0.13/1.14
245	**216**	**1.01**	0.55/0.14	**3.97**	1.3/3.4	**1.20**	0.06/1.12
300	**243**	**1.02**	0.62/0.17	**3.94**	1.0/3.1	**1.24**	0.01/1.15

Calc.: calculated; Vis: visible; NIR: near infrared.

the physical depth that photons achieve as they interrogate the tissue volume. In spite of the presence of this error, the corrected melanin concentration falls within only a few percent of the actual value. This is in stark contrast to values determined directly from data acquired in the visible or near-infrared wavelength range alone. This method also demonstrates a slight improvement in accuracy for determining oxyhemoglobin concentration relative to the near-infrared data, which is largely insensitive to the melanin present in the top layer of this particular model. Deoxy-hemoglobin values, however, exhibit a slight decrease in accuracy relative to the near infrared data, though still better than the visible regime derived values. Upon further examination, the near-infrared derived deoxy-hemoglobin values are initially overestimated, indicating that there are other sources of error, such as cross-talk between oxy- and deoxy-hemoglobin signatures, as opposed to the layered geometry problem that we are addressing here that would inherently produce an underestimation of chromophore values.

3.2 *Tissue Simulating Phantom Study*

Next, two layer tissue simulating silicone phantoms were experimentally investigated with the SMoQS instrument. The method for producing these interchangeable polydimethylsiloxane (PDMS; Eager Polymers) layers is described in detail elsewhere.[17] For this particular experiment, four "epidermal" layers where prepared using titanium dioxide (Atlantic Equipment Engineers) as the scattering agent and naphthol green (Sigma) for absorption contrast. These layers vary in thickness from 150 to 350 micrometers, but contain the same concentrations of absorber and scatterer in each. The absorption coefficient at 650 nm from the naphthol green concentration in these phantoms was 0.143 mm^{-1} [with the full, layer-specific absorption spectra shown in Fig. 4(a)] and reduced scattering was 1.2 mm^{-1} at 650 nm [full spectrum shown in Fig. 4(b)]. These values were independently verified in each phantom using inverse adding-doubling methods.[18] Current production methods limit these layers to a 150 micrometer thickness, though this is not a fundamental limitation. A "dermal" phantom was also prepared using TiO_2 as the scattering agent ($\mu_s' = 2.3\ mm^{-1}$ at 650 nm); however, nigrosin (Sigma) was used for absorption contrast in this layer ($\mu_a = 0.115\ mm^{-1}$ at 650 nm). This phantom is over 2-cm thick, which is considered to be semi-infinite in relation to the depth penetration of the SMoQS technique. The selection of layer-specific dyes was not motivated to directly approximate the absorption contrast found within the skin, but rather to provide two sources of absorption contrast that contained broad and overlapping spectral features.

Four measurements were collected by the SMoQS instrument, each containing a different epidermal phantom laid on top of the single dermis simulating phantom. Air bubbles were removed between the epidermal and dermal phantoms to ensure the index of refraction conditions were matched at the interface between the two layers. Figure 4(a) shows the detected absorption values as determined by the SMoQS method. Dashed lines represent the pure spectral components of the naphthol green and nigrosin in the concentrations independently verified to be in their respective layers. The respective values for measured and layer specific scattering properties are shown in Fig. 4(b). As with the simulated data, the estimated penetration depth, l_{meas}, can be calculated directly from the determined absorption and reduced scattering coefficient values as each wavelength, Fig. 4(c). Due to the broad spectral features of the two absorbers used in the top and bottom layers, a 300 nm sliding window was used to determine the region-specific, homogeneous volume concentration of the two dyes as a function of wavelength regime. Table 2 summarizes the layer thickness and layer-specific chromophore concentrations determined (relative to the independently verified absorption values) using this two layer correction method when a 300 nm window centered at 600 and 800 nm is used. Here, a value of 100% in the concentration determination indicates that this model has determined the correct concentration of layer specific absorber in the presence of scattering and other layer optical properties. Similar to the results of the Monte Carlo simulations that were previously discussed, the determination of top layer thickness was accurate to tens of micrometers. The determined layer specific concentrations, however, produced significantly improved results relative to visible and near-infrared spectral regimes when considered alone. Not only were these values, on average, within 6.5% of the actual values, but the variance in the determined values as a function of layer thickness has also been reduced relative to visible and near-infrared spectral regimes.

4 Discussion

SMoQS measurements provide broadband optical properties at ~1 nm resolution, spanning visible and near-infrared regimes.

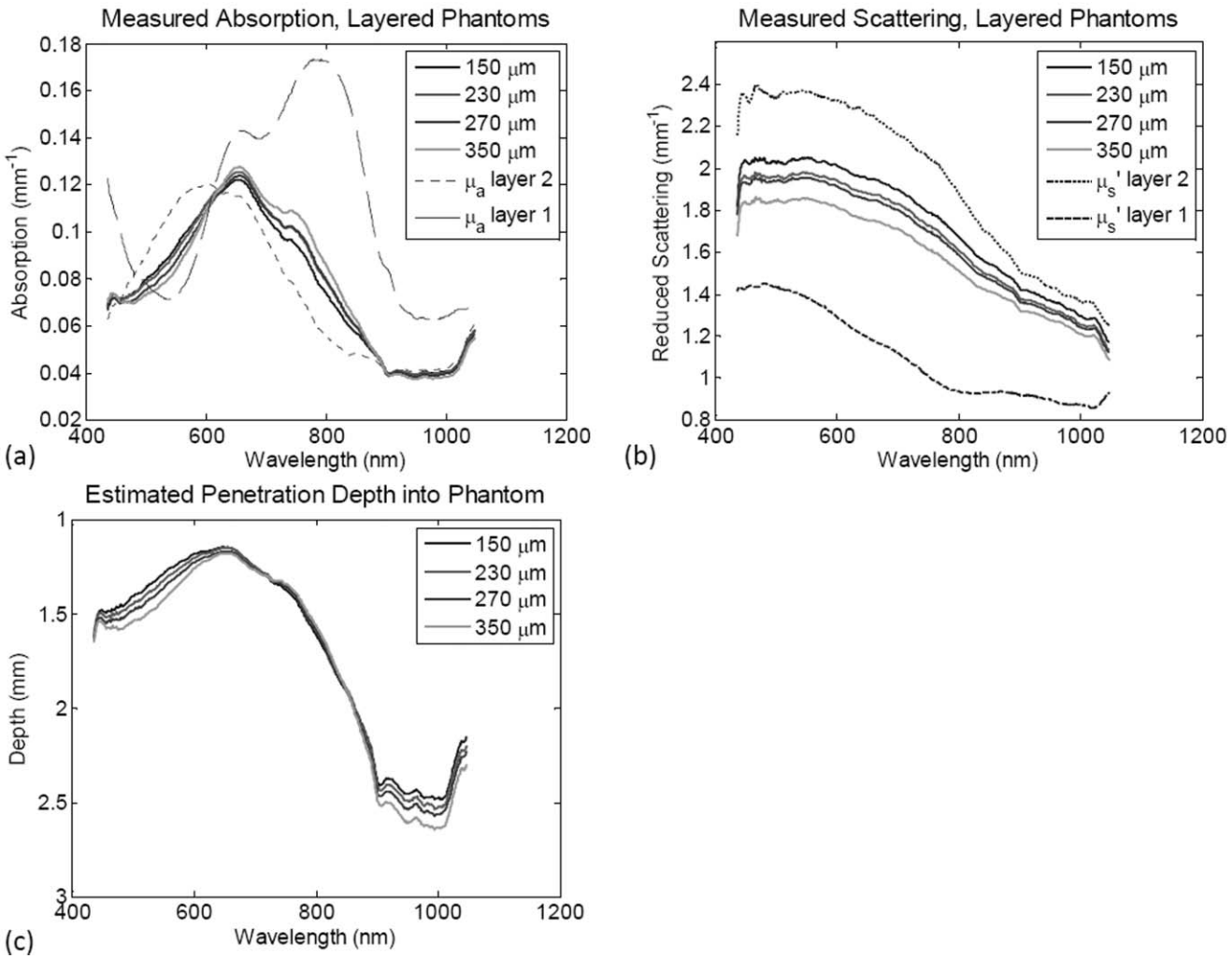

Fig. 4 Experimental results. (a) The resulting absorption spectra from the two layer phantom constructs [dashed and dotted spectra indicate the layer-specific absorption (i.e., 100% concentration)] , (b) The resulting reduced scattering spectra from the two layer phantom constructs (dashed and dotted spectra indicate the layer specific reduced scattering). (c) The calculated optical penetration depth based off of the wavelength specific determined absorption and reduced scattering values.

In the visible regime, these optical properties from skin are greater than those that typify the near-infrared, (~3 to 4 times greater scattering and ~10 times greater absorption). Thus, reflectance geometry measurements of tissue using visible light results in a relatively smaller volume interrogation compared to near-infrared light in the same measurement geometry. Through quantitative spectroscopic approaches, this differential volume of interrogation can be exploited to determine absorption properties smaller than the total volume probed.

From both simulated and experimentally derived measurements of layered structures, estimates of top layer thickness were in reasonable agreement with the actual layer thickness

Table 2 Experimental results.

Top layer thickness (μm)		Top layer concentration (%)			Bottom layer concentration (%)		
Actual	Calc.	Actual	Calc.	Vis/NIR only	Actual	Calc.	Vis/NIR only
150	**220**	100	**86.3**	15.2/6.8	100	**101.5**	65.0/90.1
230	**280**	100	**93.2**	18.5/8.5	100	**101.9**	58.9/89.2
270	**310**	100	**93.6**	20.1/9.0	100	**100.6**	53.7/86.4
350	**355**	100	**99.5**	24.4/10.9	100	**99.1**	45.3/84.5

Calc.: calculated; Vis: visible; NIR: near infrared.

(within tens of micrometers). Systemic errors were observed as a function of layer thickness, indicating that the use of the classical definition of penetration depth metric as a proxy for the depth sensitivity of the wavelength specific depth sensitivity may not be the optimal measure to reflect this property. Monte Carlo studies have been performed that examine the accuracy of penetration depth as classically defined as a function of arbitrary absorption and scattering.[19] From these studies, a look-up table can be generated to estimate depth penetration in both diffusive and nondiffusive regimes.

Estimates of layer specific chromophore concentrations produce dramatically improved results relative to homogeneous model results, even when estimates of layer thickness may err by as much as 45%. Even in the case where layer thickness estimates err to this extreme degree, concentration estimates are determined to be within 13% of the actual value. On average, in both the simulation and experimental measurements, these estimated top layer concentrations are within 6% of the actual value and the bottom layer estimates are within 2%.

Additionally, the approach presented here is successful in decoupling the confounding effect of layer thickness from that of the layer specific chromophore concentration. When just the determined concentrations from either the visible or near-infrared spectral regime are considered, these values can vary 60 to 80%, though the actual concentrations of these chromophores do not change. By applying this two layer method, this range of variation is reduced to 13.2 and 2.4% for the top and bottom layers, respectively.

It is worth mentioning that the approach discussed here is generalized and not limited to the SMoQS technique. The partial volume model proposed here may be applied to any quantitative spectroscopic technique that can determine absorption and the reduced scattering coefficient, from which a measure of depth sensitivity may be derived. High resolution spectral content is also not a requirement to implement this model. Discrete wavelengths could be employed, provided that they are capable of sufficiently separating chromophore concentrations at distinctly separate interrogation volumes. The one distinct advantage that spatial frequency domain approaches, such as SMoQS, do hold is that the planar illumination scheme permits the simplification of the model to a one-dimensional problem in terms of depth.

As mentioned before, this is inherently an empirically derived approach. The initial bulk optical properties are still determined by a method based off of a homogeneous model, however, the variance in these results are then interpreted by a two layer model. Since this initial data processing step is not fully rigorous in terms of light transport in structured media, this initial study has been focused on isolating the layer-specific absorption properties. Unlike scattering, the absorption of oxy- and dexoy-hemoglobin provide distinct spectral features that allow methods like least-squares to differentiate them from other absorbers as melanin in distinct spectral regimes. Scattering also plays a far more complex role in terms of light transport in layered structures. To that end, the measured scattering properties have been kept to a limited role in this initial method, but will be the subject of subsequent investigation. Although planar illumination models do help reduce this complexity by reducing the transport problem to a single dimension in terms of depth, determination of layer specific scattering is not currently considered in this model. The consequence of not explicitly accounting for the layer specific scattering is evidenced in the cumulative error in layer thickness determination. In the simulation, the scattering for both layers were matched. The thinnest layer thickness produced the closest agreement between actual and determined thickness, where an underestimation error increased with increased layer thickness. In the experimental study, the top layer reduced scattering coefficient was approximately 30% of that of the bottom layer. Here, the thinnest layer thickness was overestimated; however, that error decreased as layer thickness increased. This tendency is rooted in the fact that this model assumes that optical pathlength and depth are linearly correlated, however, the presence of scattering violates that linear relation since the optical pathlength is a function of scattering within the layer and not the layer thickness itself. We believe that opportunities do exist to better account for layer specific scattering properties while also refining the accuracy of layer thickness and absorption through the development of regressive models that would use this current proposed method for an initial approximation of layer-specific optical properties and then minimize the residual error between the measured data and modeled reflectance. This will be the subject of future work.

5 Conclusion

From this two layer approach, there is substantial improvement to determine concentrations specific to tissue structure and physiology rather than reporting results tied to instrumentation implementation and geometry. It also provides a substantial reduction in variance due to layer thickness, effectively decoupling the detected chromophore concentration and top layer thickness. Further development and refinement of this model to also incorporate layer specific scattering properties is warranted, however the development of a more sophisticated model would not be trivial and considerably more complex. The spirit of the work presented here is to capture a relatively simple, straightforward procedure that is immediately useful to applications in spectroscopic skin imaging, with a particular emphasis on the ability to quantify layer specific chromophore concentrations, such as melanin and hemoglobin species. In its current deployment, this model has demonstrated substantial improvement toward the determination of optical properties of tissues, such as skin, which is independent of instrumentation or the spectroscopic technique employed.

Acknowledgments

The authors gratefully acknowledge funding provided by the NIH R03 – 5R03EB012194–02: Spatially Modulated Quantitative Spectroscopy for Dermatologic Applications, NIH NCRR Biomedical Technology Research Center (LAMMP: 5P-41RR01192), and the technical support for tissue modeling from the Virtual Photonics Technology Initiative at the Beckman Laser Institute, as well as the individual efforts of post-doctoral researcher Dmitry Yudovsky.

References

1. G. M. Palmer and N. Ramanujam, "Monte-Carlo based inverse model for calculating tissue optical properties. Part 1, Theory and validation on synthetic phantoms," *Appl. Opt.* **45**(5), 1062–1071 (2006).

2. N. Rajaram, T. H. Nguyen, and J. W. Tunnell, "A lookup-table based inverse model for measuring optical properties of turbid media," *J. Biomed. Opt.* **13**(5), 050501 (2008).
3. S. H. Tseng, A. Grant, and A. J. Durkin, "*In vivo* determination of skin near-infrared optical properties using diffuse optical spectroscopy," *J. Biomed. Opt.* **13**, 014016 (2008).
4. S. H. Tseng, P. Bargo, A. J. Durkin, and N. Kollias, "Chromophore concentrations, absorption, and scattering properties of human skin *in vivo*," *Opt. Express* **17**(17), 14599–14617 (2009).
5. R. B. Saager, D. J. Cuccia, and A. J. Durkin, "Determination of optical properties of turbid media spanning visible and near infrared regimes via spatially modulated quantitative spectroscopy," *J. Biomed. Opt.* **15**(1), 017012 (2010).
6. T. H. Pham, T. Spott, L. O. Svaasand, and B. J. Tromberg, "Quantifying the properties of two-layer turbind media with frequency-domain diffuse reflectance," *Appl. Opt.* **39**(25), 4733–4745 (2000).
7. J. Weber, D. Cuccia, A. Durkin, and B. Tromberg, "Noncontact imaging of absorption and scattering in layered tissue spatially modulated structured light," *J. Appl. Phys.* **105**, 102028 (2009).
8. N. Doegnitz and G. Wagnieres, "Determination of tissue optical properties by steady-state spatial frequency-domain reflectometry," *Lasers Med. Sci.* **13**, 55–65 (1998).
9. D. J. Cuccia, F. Bevilacqua, A. J. Durkin, F. R. Ayers, and B. J. Tromberg, "Quantitation and mapping of tissue optical properties using modulated imaging," *J. Biomed. Opt.* **14**(2), 024012 (2009).
10. J. T. Whitton and J. D. Everall, "The thickness of the epidermis," *Br. J. Dermatol.* **89**, 467–476 (1973).
11. M. J. Koehler, T. Vogel, P. Elsner, K. Koenig, R. Bueckle, and M. Kaatz, "*In vivo* measurement of the human epidermal thickness in different localizations by multiphoton laser tomography," *Skin Res. Technol.* **16**, 259–264 (2010).
12. S. L. Jacques, "Simple theory, measurements, and rules of thumb for dosimetry during photodynamic therapy," *Photodynamic Therapy: Mechanisms, Proc. SPIE* **1065**, 100–108 (1989).
13. L. Wang, S. L. Jacques, and L. Zheng, "MCML – Monte Carlo modeling of light transport in multi-layered tissues," *Comput. Methods Programs Biomed.* **47**, 131–46 (1995).
14. S. L. Jacques, R. D. Glickman, and J. A. Schwartz, "Internal absorption coefficient and threshold for pulsed laser disruption of melanosomes isolated from retinal pigment epithelium." *Proc. SPIE* **2681**, 468–477 (1996).
15. S. A. Prahl, "Optical absorption of hemoglobin," *Tabulated Hemoglobin Spectra*, compiled by S A Prahl (Oregon Medical Laser Center, accessed 10 Dec. 2010). http://omlc.ogi.edu/spectra/hemoglobin/
16. S. L. Jacques, "Origins of tissue optical properties in the UVA, visible, and NIR regions," in *OSA TOPS on Advances in Optical Imaging and Photon Migration 2*, R. R. Alfano and J. G. Fujimoto, Eds., pp. 364–371, Optical Society of America, Washington, DC (1996).
17. R. B. Saager, C. Kondru, K. Au, K. Sry, F. Ayers, and A. J. Durkin, "Multilayer silicone phantoms for the evaluation of quantitative optical techniques in skin imaging," *Proc. SPIE* **7567**, 756706 (2010).
18. S. A. Prahl, M. J. C. van Gemert, and A. J. Welch, "Determining the optical properties of turbid media by using the adding-doubling method," *Appl. Opt.* **32**, 559–568 (1993).
19. S. A. Carp, S. A. Prahl, and V. Venugopalan, "Radiative transport in the delta-P1 approximation: accuracy of fluence rate and optical penetration depth predictions in turbid semi-infinite media," *J. Biomed. Opt.* **9**(3), 632–647 (2004).